

Gentle heating by mixing in cooling flows

Shlomi Hillel and Noam Soker

Department of Physics, Technion – Israel, Institute of Technology, Haifa 32000, Israel; shlomihi@tx.technion.ac.il; soker@physics.technion.ac.il

14 December 2024

ABSTRACT

We analyze three-dimensional hydrodynamical simulations of the interaction of jets and the bubbles they inflate with the intra-cluster medium (ICM), and show that the heating of the ICM by mixing hot bubble gas with the ICM operates over tens of millions of years, and hence can smooth the sporadic activity of the jets. The inflation process of hot bubbles by propagating jets forms many vortices, and these vortices mix the hot bubble gas with the ICM. The mixing, hence the heating of the ICM, starts immediately after the jets are launched, but continues for tens of millions of years. We suggest that the smoothing of the active galactic nucleus (AGN) sporadic activity by the long-lived vortices accounts for the recent finding of a gentle energy coupling between AGN heating and the ICM. *Key words:* galaxies: clusters: intracluster medium — galaxies: jets

1 INTRODUCTION

The intra-cluster medium (ICM) in cooling flows, in galaxies, groups, and clusters of galaxies, is heated by jets launched from the central active galactic nucleus (AGN) and operate via a negative feedback mechanism (e.g., Fabian 2012; McNamara & Nulsen 2012; Farage et al. 2012; Gaspari et al. 2013; Pfrommer 2013; Barai et al. 2016; for a recent review see Soker 2016). It is thought now that the feedback is closed by the *cold feedback mechanism* (Pizzolato & Soker 2005), namely, cold dense clumps that feed the AGN (e.g., some papers from the last 2 years, Gaspari 2015; Voit & Donahue 2015; Voit et al. 2015; Li et al. 2015; Prasad et al. 2015; Singh & Sharma 2015; Tremblay et al. 2015; Valentini & Brighenti 2015; Choudhury & Sharma 2016; Hamer et al. 2016; Loubser et al. 2016; Russell et al. 2016; McNamara et al. 2016; Yang & Reynolds 2016; Barai et al. 2016; Prasad et al. 2016; Tremblay et al. 2016; Donahue et al. 2017; Gaspari & Sądowski 2017; Gaspari et al. 2017; Voit et al. 2017; Meece et al. 2017). The new results of Hogan et al. (2017) suggest that the perturbations that feed the AGN should start as non-linear ones, as was suggested in the original paper by Pizzolato & Soker (2005).

Although there is a general consensus on the AGN feedback activity, there is a dispute on the exact process that transfers the energy from the jets to the ICM in this jet feedback mechanism (JFM). Heating processes that have been proposed in the literature include sound waves (e.g., Fabian et al. 2006; Fabian 2012; Fabian et al. 2017) that can be excited by jet-inflated bubbles (Sternberg & Soker 2009), shocks that are excited by the jets (e.g., Forman et al. 2007; Randall et al. 2015; for problems with shock heating see, e.g., Soker et al. 2016), heating by dissipation of ICM turbulence (e.g., De Young 2010; Gaspari et al. 2014; Zhuravleva et al. 2014; for problems and limitations of turbulent heating see, e.g., Falceta-Gonçalves et al. 2010; Reynolds et al. 2015; Hitomi Collaboration et al. 2016; Hillel & Soker 2017), cosmic rays (e.g., Fujita et al. 2013; Fujita & Ohira 2013), and mixing of hot bubble gas with the ICM (e.g., Brüggén & Kaiser 2002; Brüggén et al. 2009; Gilkis & Soker 2012; Hillel & Soker

2014, 2016; Yang & Reynolds 2016). Some processes can operate together, such as cosmic rays and thermal conduction (e.g., Guo & Oh 2008), mixing of cosmic rays from jet-inflated bubbles to the ICM (Pfrommer 2013), and heating by turbulence and turbulent-mixing (e.g. Banerjee & Sharma 2014).

The heating by mixing process is caused by the many vortices that are excited by the inflation process of the bubbles (Gilkis & Soker 2012; Hillel & Soker 2014, 2016; Yang & Reynolds 2016). A by product of this process is that the vortices induce turbulence in the ICM, accounting for the finding of turbulence in some cooling flows (e.g., Zhuravleva et al. 2014, 2015; Arévalo et al. 2016; Anderson & Sunyaev 2016; Hofmann et al. 2016).

The JFM is more complicated than what simple arguments might suggest. For example, the jets might have positive components to the feedback cycle in addition to the more influential negative one. The positive components include the interaction of the jets with the ICM that form inhomogeneities that are the seeds of future dense blobs (e.g., Pizzolato & Soker 2005), or the bubbles that through their buoyant motion lift low entropy gas that can cool and fall to feed the AGN (e.g., McNamara et al. 2016).

In the present study we refer to two recent papers, and we further emphasize the dominant role that vortices that are formed during the inflation process of the bubbles play in the feedback heating cycle of the ICM.

Sternberg & Soker (2008) show that to obtain the correct flow structure it is mandatory to inflate bubbles by jets, rather than by artificially injecting energy off-center. In a recent paper Weinberger et al. (2017) insert jets off-center. One of their conclusions is that mixing of lobe material with the ICM is sub-dominant in the heating process. In section 3 we examine the formation of vortices early on by jets injected from the center. We argue that to obtain the full power of heating by mixing, the jets should be inserted from the center.

In a new and thorough study Hogan et al. (2017) analyze the properties of 56 clusters of galaxies, and conclude that “. . .the energy coupling between AGN heating and atmospheric gas is gen-

pler than most models predict” (see also McNamara et al. 2016). In an earlier paper (Hillel & Soker 2016) we conducted three dimensional (3D) hydrodynamical simulations of intermittent jets interacting with the ICM. Each activity phase lasts for a period of 10 Myr, with a quiescence period of 10 Myr between two consecutive active phases. An interesting finding of these 3D hydrodynamical numerical simulations is that the large scale vortices continue to exist even in the quiescence periods. This implies that the mixing is a continuous process, and no large variations are expected during the evolution if the decay time of the vortices is about equal or larger than the quiescence phases period. In section 4 we show that the expectation of the heating by mixing process and the new findings of Hogan et al. (2017) are compatible with each other.

We summarize our claims in section 5. We will present results from our earlier simulations, but the analysis extends to a new domain. We open by describing our numerical scheme in section 2.

2 NUMERICAL SETUP

We present results from our earlier 3D hydrodynamical numerical simulations (Hillel & Soker 2016), where we used the numerical code PLUTO (Mignone et al. 2007). We further analyzed these simulations in our study of the galaxy group NGC 5813 (Soker et al. 2016), and in our interpretation of the Hitomi observations of the Perseus cluster of galaxies (Hillel & Soker 2017). We here describe only the essential features of the numerical scheme

The computational grid is in the octant where the three coordinates x , y and z are positive, and the z axis is chosen along the symmetry axis of the jet. The $z = 0$ plane is a symmetry plane where we apply reflective boundary conditions. The highest resolution of the adaptive mesh refinement is ≈ 0.1 kpc.

We inject the jet from a circle $\sqrt{x^2 + y^2} \leq 3$ kpc at the plane $z = 0$, and with a half-opening angle of $\theta_j = 70^\circ$. The initial jet velocity is $v_j = 8200$ km s $^{-1}$. The jet is periodic in time. It is injected continuously for a period of 10 Myr, starting at $t = 0$, followed by an off-phase that lasts for 10 Myr. Namely, the jet-active phases are in the time intervals

$$20(n-1) \leq t_n^{\text{jet}} \leq 10(2n-1), \quad n = 1, 2, 3, \dots \quad (1)$$

The mass deposition rate into the two opposite jets (only one is simulated, or more accurately, only quarter of a jet is simulated) and the power of the two jets during each on-episode are $\dot{M}_{2j} = 2\dot{E}_{2j}/v_j^2 = 94M_\odot \text{ yr}^{-1}$ and $\dot{E}_{2j} = 2 \times 10^{45} \text{ erg s}^{-1}$, respectively.

The initial density of the ICM in the grid is set to be (e.g., Vernaleo & Reynolds 2006)

$$\rho_{\text{ICM}}(r) = \frac{\rho_0}{[1 + (r/a)^2]^{3/4}}, \quad (2)$$

with $a = 100$ kpc and $\rho_0 = 10^{-25} \text{ g cm}^{-3}$. The initial ICM temperature is $T_{\text{ICM}}(0) = 3 \times 10^7 \text{ K}$. We include a gravity field that maintains an initial hydrostatic equilibrium, and we keep it constant in time. We also include radiative cooling for a solar metallicity gas from Table 6 of Sutherland & Dopita (1993).

3 VORTICES BY JET-INFLATED BUBBLES

In Fig. 1 we present the inflation of the bubble in the first activity cycle: the jet is active in the time period 0 – 10 Myr and it is turned off for the time period 10 – 20 Myr. At $t = 20$ Myr the second activity cycle starts (eq. 1). We present the density (left column)

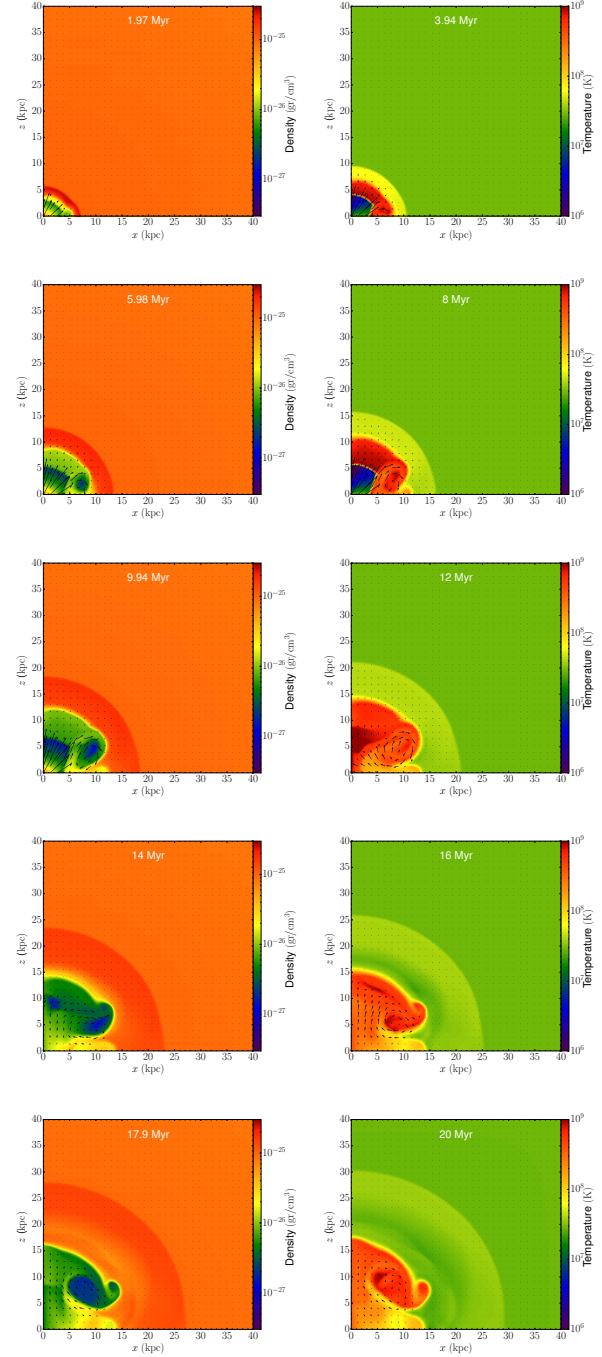


Figure 1. Early evolution of the flow velocity and either temperature of density, presented in the $y = 0$ meridional plane at the first jet’s activity cycle. The color scales of the temperature and the density are in logarithmic scales. Arrows show the velocity, with length proportional to the velocity magnitude. A length of 1 kpc on the map corresponds to 1700 km s^{-1} . When the jet is active, the length of arrows close to the origin corresponds to 8200 km s^{-1} .

and temperature (right column) in color-contours, and the velocity vectors by arrows, in the meridional plane $y = 0$ at 10 times as indicated in the figure.

Fig. 1 clearly shows the rapid development of vortices inside and outside the jet-inflated hot bubble. The rapid development of vortices can be understood as follows. Although a large shear exists

between the fast jet and the static ICM, the vortices are mainly formed in the post-shock region. As the jet's material hits the ICM it is shocked. A very high pressure region is formed in the post-shock region. The distance from the center of this high-pressure region increases with time as the jet continues to be active. The post-shock gas expands rapidly to the sides of that region, i.e., about perpendicular to the original direction of the gas. It then expands backward, to form what is termed the cocoon, i.e., shocked jet's material that lags behind the jet. This motion to the side and then backward forms large vortices. The outward motion of the high pressure region and the vortex that it forms can be best seen by following the low-density region (that is a cross section of a low density volume) at the center of the vortex on the $y = 0$ plane. This low-density region is the blue-color region moving from about $(x, z) = (7, 2)$ kpc at $t = 6$ Myr to about $(x, z) = (9, 7)$ kpc at $t = 18$ Myr.

The lower right panel of Fig. 1 shows that even 10 Myr after the jets has been turned off ($t = 20$ Myr) the temperature is not smoothed yet. This implies that the vortices did not completely mix yet the hot bubble gas and the ICM. We see also that the vortices, in particular the large vortex, still exist and they continue the mixing process. We discuss this in detail in section 4 below.

The simulation of a propagating jet is essential to capture the formation of the vortices. Jets that encounter an ambient gas excite vortices even when the medium is homogenous, rather than stratified. When an artificial bubble or jet is inserted at zero velocity off-center, on the other hand, vortices might be formed only as a result of the upward motion of the hot region due to buoyancy. In an homogeneous medium artificial bubbles will form no vortices. Other limitations of artificially introduced jets and bubbles are discussed by Sternberg & Soker (2008).

Let us summarize and further emphasize the analysis of our simulations in this section. The many vortices that are formed by the shocked jets and the bubble-inflation process play a crucial role in heating the ICM and in determining the properties of the feedback cycle, not only in cooling flows, but in other environments as well (Soker et al. 2013; Soker 2016). To obtain these vortices the numerical simulations must include propagating jets that start from the center. Simulations that inject static hot gas or jets off-center might lead to inaccurate conclusions. In a recent paper Weinberger et al. (2017) insert jets off-center. We think that this is the reason that they find that mixing of material from the bubbles with the ICM is not the main heating mechanism of the ICM. When we inject jets from the center, we find heating by mixing to be the main heating mechanism of the ICM (Hillel & Soker 2016).

4 LONG LIVED VORTICES

Motivated by the new results of Hogan et al. (2017) and McNamara et al. (2016), in this section we show that heating by mixing operates in a gentle manner. In Fig. 2 we present the flow structure of the fifth activity cycle in the meridional plane $y = 0$. The jet is turned on for the fifth time during the time period 80 – 90 Myr, followed by a 10 Myr quiescence period, 90 – 100 Myr. It is the quiescence period that we are interested in here. We present the density and temperature at $t = 80$ Myr, that is, 10 Myr after the end of the fourth active phase and at the beginning of the fifth active phase (eq. 1), followed by eight later times where we present either the density (left column) or the temperature (right column). In all panels we present the velocity map.

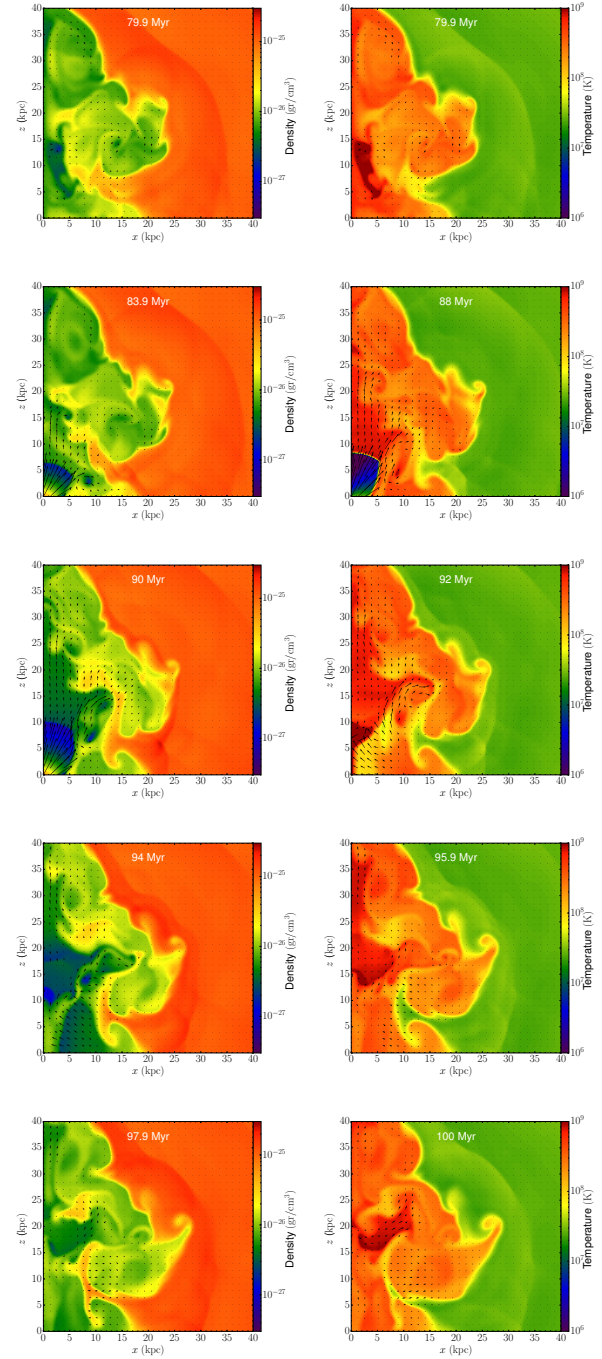


Figure 2. Density, temperature and velocity maps during the fifth activity cycle. The jet is active for the fifth time in the time period 80 – 90 Myr. Arrows show the velocity, with length proportional to the velocity magnitude. A length of 1 kpc on the map corresponds to 1700 km s^{-1} . When the jet is active, the length of arrows close to the origin corresponds to 8200 km s^{-1} .

In addition to the velocity maps, in Fig. 3 we follow the spreading of the gas injected in the jet by presenting the tracer of the jet's material. The tracer is a non-physical mark that is frozen-in to the flow, and indicates the spread of the material over time. We set the initial value of the tracer of the gas that is injected into the jet to be $\xi_j(0) = 1$, and set $\xi_j(0) = 0$ for the ICM. At later times the value of $\xi_j(t)$ in each grid cell represents the fraction of the gas that started in the jet.

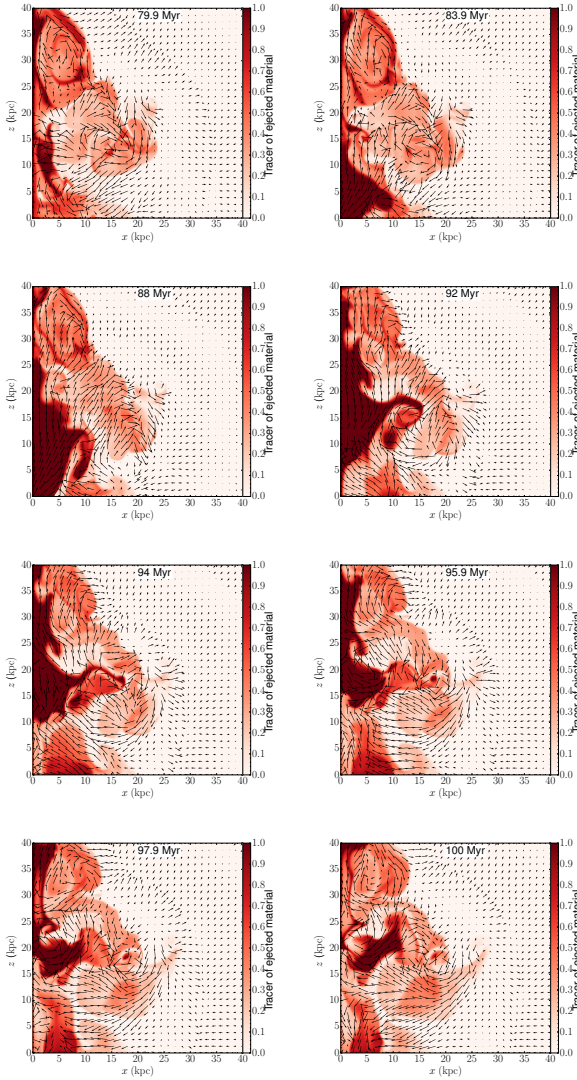


Figure 3. Evolution with time of the gas that is injected in the jet and the flow map in the meridional plane $y = 0$. The color coding is for the fraction $\xi_j(t)$ at each grid point of the gas that originated in the jet. The largest velocity vector corresponds to $v_m = 400 \text{ km s}^{-1}$, a Mach number of about 0.5. Higher velocities are marked with arrows with the same length as that of v_m .

We set the velocity scale in Fig. 3 to emphasize the flow in the ICM rather than of the post-shock jet’s material, hence the velocity scale is different than in Figs. 1 and 2. The vortices mix the shocked jet’s material with the ICM. We take this mixing to be the main heating process of the ICM (Hillel & Soker 2016). From the fluctuating values of the tracer of the jets ξ_j , even 10 Myr after the jet has been turned off (both at $t = 80 \text{ Myr}$ and $t = 100 \text{ Myr}$), we learn that the bubbles’ gas is not fully mixed with the ICM. The vortices are still strong and the mixing process is going on. This is also seen from the non-smooth temperature maps presented in Fig. 2.

The conclusion from the tracer and temperature fluctuations even 10 Myr after the jet has been turned off, and the ongoing vortex activity, is that the heating by mixing is a continuous process that takes place on a relatively long time scale. The mixing-heating smooths out the sporadic activity of the jets launched by the AGN.

This, we propose, explains the finding reported by Hogan et al. (2017) and McNamara et al. (2016) of a gentle heating of the ICM in cooling flow clusters.

In the past we studied the mixing-heating by conducting 2D numerical simulations (Gilkis & Soker 2012; Hillel & Soker 2014). In those simulations each vortex is actually a torus because the imposed axi-symmetry of the grid, and hence the results are less accurate in describing vortices. Nonetheless, we can see that the vortices live for more than 60 Myr after the jets have been turned off at $t = 20 \text{ Myr}$ (figure 6 in Gilkis & Soker 2012 and figures 3-5 in Hillel & Soker 2014). These results of 2D simulations, although less accurate for vortices, strengthen the finding of the present analysis. Future studies should examine the behaviour of vortices during such long quiescence periods but in full 3D simulations, and for different jets’ properties.

One limitation of our simulation is that it does not include physical viscosity that dissipates the kinetic energy of the vortices. We have only numerical dissipation. It is reasonable to assume that the largest vortices live for at least one revolution time $\tau_r \simeq \pi D/v$, where D is the typical size of the largest vortices and v is their rotational velocity. Substituting typical values for the largest vortices of $D \simeq 10 \text{ kpc}$ and $v \simeq 200 \text{ km s}^{-1}$, we find $\tau_r \approx 10^8 \text{ yr}$. This is long enough to keep the turbulence significance even during the AGN-quiescence time periods.

5 SUMMARY

We have analysed some properties of a 3D hydrodynamical simulation of jet intermittent activity in a cooling flow cluster. This simulation was analyzed in three earlier studies (Hillel & Soker 2016; Soker et al. 2016; Hillel & Soker 2017). In the present paper we extended the analysis and concentrated on the onset of the vortices and on the long time scale over which the vortices mix the hot bubble gas with the ICM.

In section 3 we strengthened the claim of Sternberg & Soker (2008) that to reveal the full properties of the jet-ICM interaction it is necessary to simulate the formation and evolution of hot bubbles by injecting propagating jets from the center of the cluster. In Fig. 1 we showed that the propagating jets form large and vigorous vortices already very close to the center. Such vortices close to the center are not formed when jets or bubbles are inserted off-center. We think that the finding of Weinberger et al. (2017) that mixing is not the main heating process of the ICM might result from that they insert jets off-center, rather than from the center.

Based on our earlier results (e.g., Hillel & Soker 2016) we argue that mixing hot bubble gas with the ICM is the main heating process of the ICM. In section 4 we followed the mixing process, concentrating on the quiescence period 90 – 100 Myr. From Fig. 2 that presents fluctuations in the temperature near the center, and from Fig. 3 that presents the fluctuations in the concentration of gas that originated in the jet, we learn that even 10 Myr after the jets has been turned off the mixing is not complete. We also see in these figures that the vortices still exist at that time. These imply that the heating by mixing process operates over a long time, and it smooths the large variations in the power of the AGN. We argued that this explains the finding reported by Hogan et al. (2017) and McNamara et al. (2016) of a gentle heating of the ICM in cooling flow clusters.

This research was supported by the Pazy Foundation.

REFERENCES

- Anderson, M., E., & Sunyaev, R. 2016, arXiv:1506.01703
- Arévalo, P., Churazov, E., Zhuravleva, I., Forman, W. R., & Jones, C. 2016, *ApJ*, 818, 14
- Banerjee, N., & Sharma, P. 2014, *MNRAS*, 443, 687
- Barai, P., Murante, G., Borgani, S., Gaspari, Massimo., Granato, G. L., Monaco, P., & Ragone-Figueroa, Cinthia 2016, *MNRAS*, 461, 1548
- Brüggen, M., & Kaiser, C. R. 2002, *Nature*, 418, 301
- Brüggen, M., Scannapieco, E., & Heinz, S. 2009, *MNRAS*, 395, 2210
- Choudhury, P. P., & Sharma, P. 2016, *MNRAS*, 457, 2554
- De Young, D. S. 2010, *ApJ*, 710, 743
- Donahue, M., Connor, T., Voit, G. M., & Postman, M. 2017, *ApJ*, 835, 216
- Fabian, A. C. 2012, *ARA&A*, 50, 455
- Fabian, A. C., Sanders, J. S., Taylor, G. B., Allen, S. W., Crawford, C. S., Johnstone, R. M., & Iwasawa, K. 2006, *MNRAS*, 366, 417
- Fabian, A. C., Walker, S. A., Russell, H. R., Pinto, C., Sanders, J. S., & Reynolds, C. S. 2017, *MNRAS*, 464, L1
- Falceta-Gonçalves, D., de Gouveia Dal Pino, E. M., Gallagher, J. S., & Lazarian, A. 2010, *ApJ*, 708, L57
- Farage, C. L., McGregor, P. J., & Dopita, M. A. 2012, *ApJ*, 747, 28
- Forman, W., Jones, C., Churazov, E., et al. 2007, *ApJ*, 665, 1057
- Fujita, Y., Kimura, S., & Ohira, Y. 2013, *MNRAS*, 432, 1434
- Fujita, Y., & Ohira, Y. 2013, *MNRAS*, 428, 599
- Gaspari, M. 2015, *MNRAS*, 451, L60
- Gaspari, M., Brighenti, F., & Ruszkowski, M. 2013, *Astronomische Nachrichten*, 334, 394
- Gaspari, M., Churazov, E., Nagai, D., Lau, E. T., & Zhuravleva, I. 2014, *A&A*, 569, A67
- Gaspari, M., & Sądowski, A. 2017, *ApJ*, 837, 149
- Gaspari, M., Temi, P., & Brighenti, F. 2017, *MNRAS*, 466, 677
- Gilkis, A., & Soker, N. 2012, *MNRAS*, 427, 1482
- Guo, F., & Oh, S. P. 2008, *MNRAS*, 384, 251
- Hamer, S. L., Edge, A. C., Swinbank, A. M., et al. 2016, *MNRAS*, 460, 1758
- Hillel, S., & Soker, N. 2014, *MNRAS*, 445, 4161
- Hillel, S., & Soker, N. 2016, *MNRAS*, 455, 2139
- Hillel, S., & Soker, N. 2017, *MNRAS*, 466, L39
- Hitomi Collaboration 2016, *Nature*, 535, 117
- Hofmann, F., Sanders, J. S., Nandra, K., Clerc, N., & Gaspari, M. 2016, *A&A*, 585, A130
- Hogan, M. T., McNamara, B. R., Pulido, F., et al. 2017, arXiv:1704.00011
- Li, Y., Bryan, G. L., Ruszkowski, M., Voit, G. M., O'Shea, B. W., & Donahue, M. 2015, *ApJ*, 811, 73
- Loubser, S. I., Babul, A., Hoekstra, H., Mahdavi, A., Donahue, M., Bildfell, C., & Voit, G. M. 2016, *MNRAS*, 456, 1565
- McNamara, B. R., & Nulsen, P. E. J. 2012, *New Journal of Physics*, 14, 055023
- McNamara, B. R., Russell, H. R., Nulsen, P. E. J., Hogan, M. T., Fabian, A. C., Pulido, F., & Edge, A. C. 2016, *ApJ*, 830, 79
- Meece, G. R., Voit, G. M., & O'Shea, B. W. 2017, arXiv:1603.03674
- Mignone, A., Bodo, G., Massaglia, S., et al. 2007, *ApJS*, 170, 228
- Pfrommer, C. 2013, *ApJ*, 779, 10
- Pizzolato, F., & Soker, N. 2005, *ApJ*, 632, 821
- Prasad, D., Sharma, P., & Babul, A. 2015, *ApJ*, 811, 108
- Prasad, D., Sharma, P., & Babul, A. 2016, arXiv:1611.02710
- Randall, S. W., Nulsen, P. E. J., Jones, C., et al. 2015, *ApJ*, 805, 112
- Reynolds, C. S., Balbus, S. A., & Schekochihin, A. A. 2015, *ApJ*, 815, 41
- Russell, H. R., McNamara, B. R., Fabian, A. C., et al. 2016, *MNRAS*, 458, 3134
- Singh, A., & Sharma, P. 2015, *MNRAS*, 446, 1895
- Soker, N. 2016, *New Astronomy Reviews*, in press, arXiv:1605.02672
- Soker, N., Akashi, M., Gilkis, A., Hillel, S., Papish, O., Refaelovich, M., & Tsebrenko, D. 2013, *Astronomische Nachrichten*, 334, 402
- Soker, N., Hillel, S., & Sternberg, A. 2016, *Research in Astronomy and Astrophysics*, 16, 015
- Sternberg, A., & Soker, N. 2008, *MNRAS*, 389, L13
- Sternberg, A., & Soker, N. 2009, *MNRAS*, 395, 228
- Sutherland, R. S., & Dopita, M. A. 1993, *ApJS*, 88, 253
- Tremblay, G. R., O'Dea, C. P., Baum, S. A., et al. 2015, *MNRAS*, 451, 3768]
- Tremblay, G. R., Oonk, J. B. R., Combes, F., et al. 2016, *Nature*, 534, 218
- Valentini, M., & Brighenti, F. 2015, *MNRAS*, 448, 1979
- Vernaleo, J. C., & Reynolds, C. S. 2006, *ApJ*, 645, 83
- Voit, G. M., & Donahue, M. 2015, *ApJ*, 799, L1
- Voit, G. M., Donahue, M., Bryan, G. L., & McDonald, M. 2015, *Nature*, 519, 203
- Voit, G. M., Meece, G., Li, Y., O'Shea, B. W., Bryan, G. L., & Donahue, M. 2017, arXiv:1607.02212
- Weinberger, R., Ehlert, K., Pfrommer, C., Pakmor, R., & Springel, V. 2017, arXiv:1703.09223
- Yang, H.-Y. K., & Reynolds, C. S. 2016, *ApJ*, 829, 90
- Zhuravleva, I., Churazov, E., Arevalo, P., et al. 2015, *MNRAS*, 450, 4184
- Zhuravleva, I., Churazov, E., Schekochihin, A. A., et al. 2014, *Nature*, 515, 85